JOURNAL OF AIRCRAFT
Vol. 44, No. 6, November–December 2007

Bending of Bonded Composite Repairs for Aluminum Aircraft Structures: A Design Study

Randal J. Clark* and Douglas P. Romilly†
University of British Columbia,
Vancouver, British Columbia V6T 1Z4, Canada

DOI: 10.2514/1.30895

This paper describes an experimental and finite element study of a bonded composite repair applied to a metallic aircraft structure. The experimental study involves the fatigue testing and fractographic examination of 2024-T3 aluminum plates repaired with boron/epoxy composite patches. The two plates are tested simultaneously in a sandwich panel configuration with and without an aluminum honeycomb spacer to provide bending restraint. The specimen was heavily instrumented, with strains being measured on the surface of the patch at many locations, thus allowing the validation of a three-dimensional finite element model and an assessment of the effects of geometrically nonlinear bending, buckling, and crack closure on the mechanical response and strength of the repair. The experimental and finite element results illustrate the important influence of bending and composite failure modes on the life and strength of the repair. The authors use the experimental results and the validated finite element analysis to evaluate the effectiveness of the methods and data currently available in the open literature for damage-tolerance substantiation, and then, by applying probabilistic methods and the principle of compounded conservatism to the findings, propose a new process for classifying bonded repairs and assigning requirements for testing and inspections.

Nomenclature

a	=	crack length
E	=	Young's modulus
G	=	shear modulus or strain energy release rate
K	=	stress-intensity factor
p	=	pressure
r	=	radius of the patch
t	=	thickness
α	=	coefficient of thermal expansion
ν	=	Poisson's ratio
σ	=	normal stress
τ	=	shear stress

Subscripts

a	=	adhesive property
b	=	bending
m	=	membrane
p	=	plate property
I	=	opening mode
II	=	sliding mode

I. Introduction

A BONDED composite patch is a fiber-reinforced epoxy doubler used to reinforce weak structure or repair cracked aircraft structure. The patch acts both to reduce stresses in the underlying structure and to restrict the opening of cracks that may lie beneath the structure. These effects and the smooth load transfer inherent to bonding offer the potential for a significant increase in fatigue life when compared with mechanically fastened repairs (shown in Fig. 1). The technology also offers improvements in cost, weight, and inspectability. The main barrier to the widespread use of this technology is the lack of a comprehensive process for damage-tolerance analysis, particularly regarding the mechanical assessment of the structure in the presence of significant bending loads, which can lead to early failure. The other significant impediment is the assurance of bond durability for repairs applied in a maintenance and repair facility.

Many experiments have been performed to investigate failure mechanisms, to demonstrate the predictive performance of models, and to evaluate repair materials and the mechanical phenomena in a repair. The test article used in this study is the widely used Australian Aeronautical and Maritime Research Laboratories (AMRL) specimen. It consists of two repaired plates that are bonded to an aluminum honeycomb support to restrict the bending induced by the neutral axis offset of the repair and to model the support of underlying structures that often exist in the highly stressed regions of an aircraft. Baker presented results for the AMRL specimen that illustrate the effects of cure-cycle parameters [1,2], disbonding [1,3], patch shear deformation [2,4], adhesive plasticity [4], and test temperature [1] on performance. In Canada, the AMRL specimen has been used by the National Research Council of Canada Institute for Aerospace Research (NRC-IAR) to examine the effects of load spectrum, compressive loading, and adverse environments on patch performance [5,6], and it has been used by Albat et al. [7] to evaluate thermal strains. With the honeycomb bending restraint, the failure mode of the repair has consistently been the continued cracking of the aluminum with accompanying adhesive disbonding. Double lap-shear hybrid bonded joint specimens matching the composition and geometry of the AMRL specimen geometry have been used to investigate the effects of patch shear deformation and adhesive plasticity on the apparent stiffness of the patch in the region of the crack [4], to determine the rate of disbonding in the region of the crack [8], and to examine disbonding at the edges of the repair. Patch shear deformation and adhesive plasticity have been shown to reduce patch life by reducing the restraint against crack opening imposed by the repair [4]. It has also been shown that increasing the cure-cycle temperature and time can impose two penalties on patch performance:

1) Tensile thermal residual stresses from a mismatch in thermal expansion coefficients can accelerate fatigue crack growth.

Received 8 March 2007; revision received 9 July 2007; accepted for publication 17 July 2007.

*Ph.D. Candidate, Department of Mechanical Engineering, 2054-6250 Applied Science Lane. Student Member AIAA.

†Associate Professor, Department of Mechanical Engineering, 2054-6250 Applied Science Lane. Member AIAA.

2) Crack growth retardation is reduced due to annealing of crack-tip plasticity-induced residual stresses.

Sharp et al. [9] also examined the effects of adhesive infiltration into the crack, which was found to increase the stress required to open the crack and hence improve fatigue life.

Other researchers have examined both similar and distinctly different types of specimens to assess the effects of bending on the life of a repair. Poole et al. [10] investigated fatigue damage propagation in thick aluminum plates repaired with graphite/epoxy patches to investigate failure modes and assess fatigue life. Similar to the AMRL specimen, repaired plates were bonded to a honeycomb core and tested in pairs to restrict bending. They examined the effect of the FALSTAFF loading spectrum on repair performance and compared the results to boundary element analyses that included the effects of adhesive plasticity. The results showed improvements on life by a factor of 3.2 for the FALSTAFF spectrum-loaded specimen and up to a factor of 17 for a constant-amplitude cyclically loaded specimen when compared with an unrepaired sheet. Denney and Mall [11–13] investigated boron/epoxy repairs applied to a single side of a thin center-cracked aluminum panel (i.e., an unbalanced repair), for which patch bending is a significant factor, due to an offset of the neutral axis. They investigated the effect of variously sized disbonds at different locations within the repair and concluded that disbonds over the crack reduce patch life, whereas disbonds away from the crack are not detrimental. They suggested that disbonds away from the crack may actually increase patch life by reducing the apparent size and stiffness of the patch and hence the amount of load it attracts from the surrounding structure. During this testing, failure occurred due to crack growth in the aluminum and little disbonding was noted. Klug et al. [14] performed a similar test using both thick and thin unbalanced repairs and noted significant disbonding near the crack and near the edges of the patch for a thick repair and only near the crack for a thin repair. For these specimens, the patch was not tapered, leading to increased stresses about the edge of the repair. In more recent work, Sabelkin et al. [15] performed tests to investigate the effects of a supporting stringer on the life of a single-sided repair applied to a thin cracked aluminum plate. Their results show that the stiffeners have an important role in reducing the stress intensity and that the thermal residual stresses must be accurately evaluated. As previously observed for repair of thin plates, they found that disbonding extended only a few millimeters from the edge of the crack.

Jones, et al. [16] presented a thorough review of the failure modes and locations of damage experienced in laboratory and military use of bonded repairs. Although most of the work reported in the literature examines the primary failure modes of the repair (i.e., substrate cracking and accompanying cohesive disbonding of the adhesive), Jones et al. stated that any damage-tolerance assessment must also include composite failure modes such as fiber failure, adhesive failure, cohesion failure at the patch-adhesive interface, adhesive failure at the adhesive-substrate interface, and interlaminar failure and delamination. In practice, unexpected failure due to crack growth and disbonding about the crack has not been a problem, because mitigation of this form of crack growth is the primary design goal of the repair and it is well accounted for in the analysis, testing, and inspection regimes. Another important factor is that the technology has mainly been limited to double-sided repairs of flat plates, to structures with bending restraint, and to structures with residual strength. Accordingly, unexpected composite failures have usually only occurred during laboratory testing for evaluation of a repair, rather than during service. The FAA [17] identifies the failure modes and locations of damage that must be considered and requires the assessment of the effects of impact damage, interply delamination, and disbonding on the composite, adhesive, and substrate.

This paper describes a unique experimental study investigating the bending mechanics of a bonded composite structural repair tested with and without bending restraint. The specimen is relatively thick and is repaired with a patch of suboptimal planar dimensions, an extreme case that allows the authors to assess the potential effects of induced bending on early failure of the structure. The specimen was composed of two edge-cracked aluminum panels, each repaired with a boron/epoxy patch and joined together as an aluminum honeycomb sandwich. Strain results are reported for the fatigue-damaged specimen under both tensile and compressive applied loading and before and after removal of the honeycomb separating the aluminum panels. Strain data from gauges fitted to the surface of the repair in the region of the crack are used to validate a three-dimensional finite element model, allowing the calculation of the stress intensity and the stresses in the adhesive and the patch as it acts to reinforce the cracked plate. Fractographic examination of the failure surfaces of the cracked plate and the composite patch illustrate the failure mechanisms active in a bending repair. It is shown that geometrically nonlinear bending and stress stiffening have a significant role in the type of failure and rate of damage, thus increasing the rate of failure. Finally, the authors use the finite element stress intensity factor, adhesive stresses, and composite stresses near the repaired crack to calculate the residual strength of the repair and rate of damage progression in light of the failure modes observed during the fatigue test. It is shown that significant problems remain for the damage-tolerance assessment of repairs, particularly in the characterization of the observed composite and adhesive failure modes.

II. Experimental Study

The experimental study involves the fatigue testing of a symmetrical honeycomb sandwich structure composed of two edge-cracked aluminum panels, each repaired with a boron/epoxy patch, as shown in Figs. 2–4. The two repaired plates are joined by a bonded aluminum honeycomb core. This specimen was originally developed by the AMRL and has also been used extensively by the NRC-IAR. As described in the Introduction, the AMRL specimen has seen extensive use in the evaluation of the bonded composite repair technology for balanced or symmetric double-sided repairs. Without bending, the failure mode has consistently been found to be the continued cracking of the aluminum with accompanying adhesive disbonding. In this study, the authors test the specimen with and without the honeycomb bending restraint to 1) investigate the failure mechanics of a repair under bending and 2) collect strain data to validate models of bending repairs. It should be noted that the AMRL specimen was designed to plates that are supported by underlying structures (e.g., ribs, stringers, etc.), and if it were designed as a

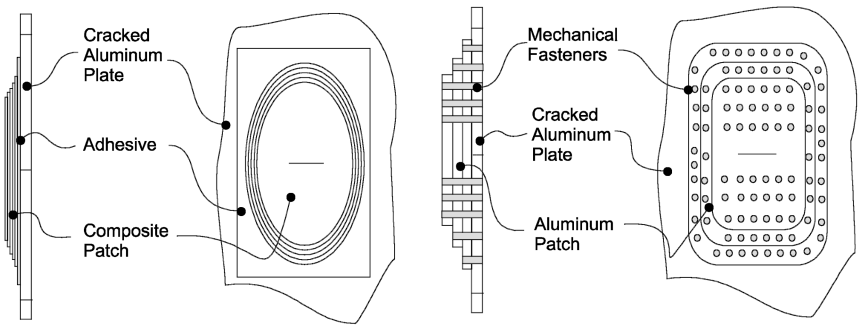

Fig. 1 A bonded repair and a mechanically fastened repair.

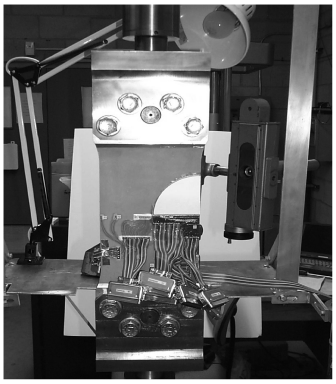

Fig. 2 Experimental apparatus.

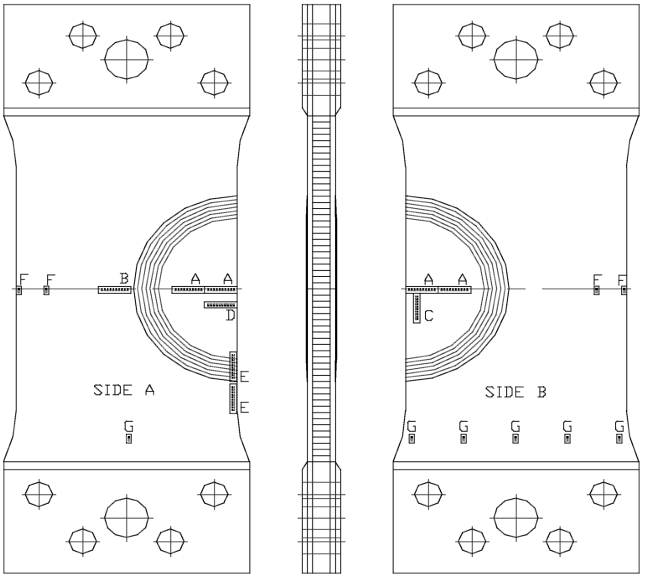

Fig. 3 Strain gauge locations.

Fig. 4 Bending under tension (left) and compression (right).

one-sided (unbalanced) repair, a larger patch would be used to reduce induced bending. As such, this fatigue test is an extreme test of the technology.

Figure 2 shows a picture of the instrumented patch and the testing apparatus. A photoelastic coating was applied to the upper half of one of the patches to reveal the distribution of stresses and estimate the extent of disbonding. An alternating-current potential drop probe was used to estimate the crack length. Unfortunately, the utility of the potential drop probe was greatly affected by significant electrical contact between the honeycomb core and the aluminum face sheets, which were electrically insulated in the original specimens built by the AMRL. A traveling microscope was used to estimate the degree of disbonding at the edge of the patch. To investigate the stress distribution within the repair, strain gauges were applied to the specimen by technicians at the NRC-IAR.

The specimen contains 100 strain gauges, most in 10-gauge strips, located as shown in Fig. 3. Engineering drawings illustrating the type, orientation, and location of the gauges are included in [18]. This paper will mainly provide results for the gauges located above the repaired crack (location A), because these strains have the greatest influence on cracking and disbonding. The gauges at location B allow the examination of the stresses about the edges of the repair, and the gauges at locations C and D allow the evaluation of the strains in the region of a disbond over the crack as it grows during fatiguing of the specimen. The gauges at location E allow the measurement of the strains in the tapered region of the repair and the stresses at the apex of the patch, where a stress concentration in the aluminum plate is known to exist. The remaining gauges allow the assessment of the distribution of the strains in the structure and allow the analyst to evaluate the grip boundary conditions. Note that the gauges will, in general, over-report any strains caused by bending, because the thickness of the gauge and the adhesive used to bond it to the structure is significant, particularly when the gauge is applied to the surface of a disbonded portion of the repair, which is fairly thin ($\sim$1 mm). This effect was taken into consideration during subsequent analysis of the measured strain data.

The applied load is reported in terms of the remote applied stress in the aluminum plate. The AMRL specimen was fatigue-loaded at 3 Hz to a maximum remote applied stress of 138 MPa at an applied stress ratio of $R = 0.1$. Strain measurements were taken at several stages, including at the start of the test and after 175,000 cycles, at which point the honeycomb spacer was removed to evaluate bending of an unrestrained patch. The initial fatigue precrack length was 19.9 mm, and the crack length when the honeycomb was removed was 45 mm, as measured by fractographic examination. Also at 175,000 cycles, isopropyl alcohol and ink were injected into the disbonded region, revealing an adhesive disbond length of approximately 5 to 6 mm from each side of the crack. Strains were measured during static testing using a Schlumberger Solartron Orion data logger, 10 gauges at a time, using a three-wire strain gauge connection. During each measurement, the strain readings at each location were taken for remotely applied plate stresses ranging from 138 to -55 MPa with the honeycomb support, and from 138 to -28 MPa without the honeycomb support. This allowed the evaluation of the nonlinear bending and the buckling responses of the structure under both tension and compression loading.

Figure 4 shows the deformation of the structure under the maximum tensile and compressive loads. After removal of the honeycomb, the increase in bending is clearly visible. Under tension, the neutral axis of the cracked plate moves to the load line, resulting in large moments and accompanying peel stresses in the adhesive. Under compression, the structure bows outward and approaches collapse. This demonstrates the large influence of bending on the mechanics of a repair and illustrates the need to account for it during design.

Examination of the fracture surface also demonstrates the need to fully evaluate the effects of induced bending on a single-sided repair. Figure 5 shows the extent of the disbonding at 175,000 cycles and at failure after 185,000 cycles. The specimen failed rapidly after removal of the honeycomb spacer that provided resistance to bending.

The disbond was initiated by the failure of the adhesive that infiltrated the crack during curing, followed by cohesive disbond growth toward the adhesive/composite interface. The disbond then grew along the interface with the scrim carrier and boron fibers. Final failure occurred by simultaneous failure of the composite patch and fracture of the cracked plate. Figure 6 shows the interfacial failure surface. Fibers that failed after removal of the bending restraint remained bonded to the underlying plate and pieces of adhesive remain attached to the boron fibers, indicating high-energy failure and good interfacial bond strength.

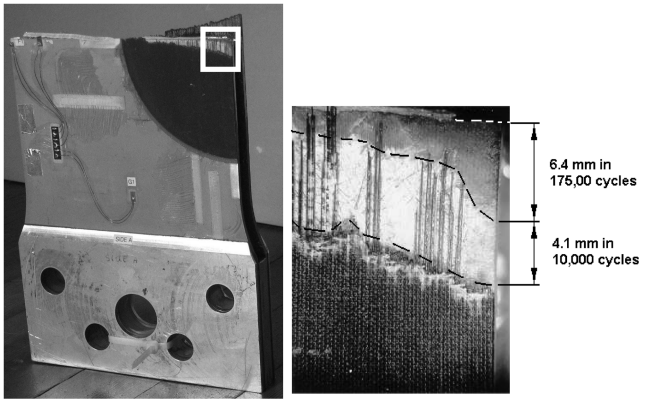

Fig. 5 Failed specimen (left) and adhesive failure surface (inset, right).

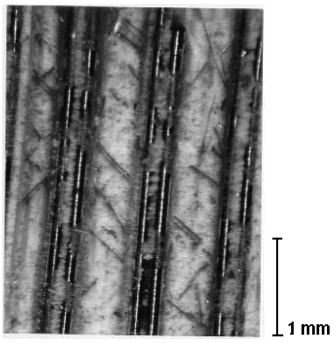

Fig. 6 Interfacial failure surface.

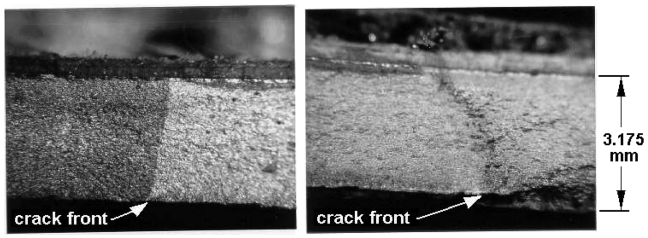

Fig. 7 The crack face after precracking (left) and after 175,000 cycles (right).

Figure 7 shows the failure surface of the aluminum plate. The left image shows the fatigue precrack and the right image shows the transition from high to low cycle fatigue after honeycomb removal at 175,000 cycles. Up to this point, the crack front grew at an angle, indicating that bending affected crack growth even before removing the honeycomb. After 175,00 cycles, the surface attains a rough appearance and shows signs of shear failure.

Selected strain measurements from this study are used in subsequent sections to validate a finite element model of the tested repair. A complete record of the strain measurements is provided in [18]. Strain results will be compared with finite element data in subsequent sections.

III. Finite Element Modeling

The authors have constructed a finite element model to simulate the experiments described earlier. The model was developed using ANSYS [19] and consists of SOLID 95 20-node brick elements with 15-node wedges at the crack tip. Table 1 shows the material properties used in the model. The seven-layer unidirectional Textron 5521 boron/epoxy prepreg composite patch is modeled as an orthotropic solid. The Cytec FM73M adhesive and 2024-T3 aluminum plate are modeled as isotropic solids, and the aluminum honeycomb spacer is modeled as an orthotropic solid with a Young's modulus of 1.86 GPa in the through-thickness direction and very low moduli in all other directions. It should be noted that there is a significant variation in the properties for the employed composite and adhesive reported by different sources. The adhesive properties used in this analysis are based upon a dry room-temperature condition and referenced later.

Table 1 Material properties and dimensions

Material	E, GPa	G, GPa	ν	α, $\infty\varepsilon/°C$	t, mm
Patch, longitudinal[a] [20]	210.0	7.24	0.21	4.61	——
Patch, transverse[a] [20]	2.5	1.0	0.019	25.87	0.924
Adhesive	2.14	0.805 [21]	0.33	50	0.25
Plate [22]	72.4	27.2	0.33	23.45	3.125
Honeycomb, longitudinal	0.001	0.001	0	23.45	——
Honeycomb, transverse	1.86	0.001	0	23.45	6.35

[a]Current manufacturer data for 5521 boron/epoxy prepreg tape is available online at http://www.specmaterials.com/5521site.htm.

Thermal residual strains imparted by the cure process and operating temperature are a very important consideration for bonded composite repairs and can be characterized by an effective stress-free temperature that accounts for creep of the adhesive and polymer matrix as the specimen is cooled during the cure cycle. For the materials systems and specimen geometry used for this experiment, using a cure temperature of 121°C, it has been shown that the effective stress-free temperature for this specimen is 81°C [7]. The experiments were conducted at room temperature (approximately 20°C) and, accordingly, a temperature difference of 61°C was applied in the finite element model.

Figure 8 is a planar view of the model, in which the inset (Fig. 8a) shows the crack-tip elements and Fig. 8b shows the aluminum substrate symmetry and pressure boundary conditions for a crack of length a and patch of radius r ($\sim$75 mm). To model the grips, the nodes on the loaded edge are also constrained to move together in the direction of the load. As in the static testing, the applied stress was varied from 138 to -55 MPa for the double-sided configuration and 138 to -28 MPa for the single-sided configuration.

The model was solved using a Newton–Raphson method with an iterative solver, large deflections, and stress stiffening. Pivot checking was disabled to allow the use of singularity elements. A user-defined macro generated singular elements that were properly oriented with respect to the crack tip and with midside nodes placed at the quarter-point position. A stress-based method was employed to calculate the stress intensity through the thickness of the plate, as described in [18]. The membrane and bending stress intensities K_m and K_b were calculated as the average stress intensity and first moment of the stress intensity through the thickness of the plate and were obtained by a linear least-squares fit to the stress intensities calculated at the integration point planes near the crack tip. Figure 9 shows a three-dimensional view of the finite element model in the region of the repaired crack, illustrating the singular crack-tip elements and the layering of the plate, adhesive, and composite patch elements.

In the next section, the model and experimental strain data are compared to demonstrate the mechanics of a repair and validate the finite element model.

IV. Validation

For validation, the finite element model was solved in an edge-cracked tension configuration, as shown in Fig. 8b. Figure 10 compares the model strain results to the longitudinal strains measured on the outside surface of the patch, as recorded before the specimen was subjected to fatigue loading. In this section, the distance x from the free edge of the repair will be referred to repeatedly and is shown in Fig. 8b. The model strains were adjusted to include the effect of gauge thickness, because the sensing element

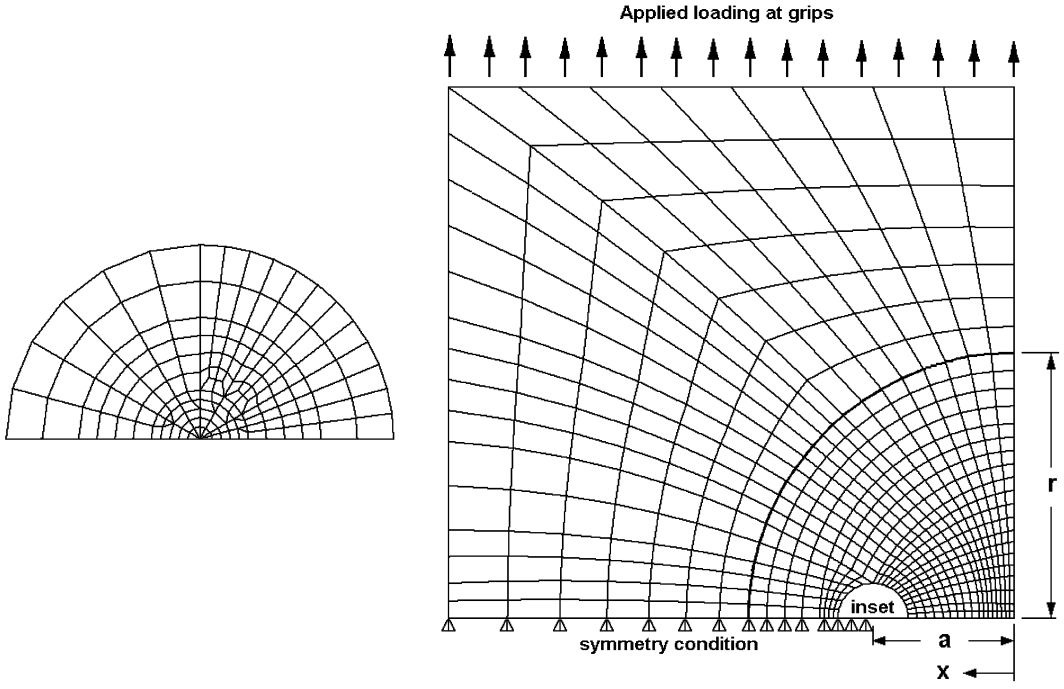

Fig. 8 Finite element mesh for a) the crack tip and b) the entire model.

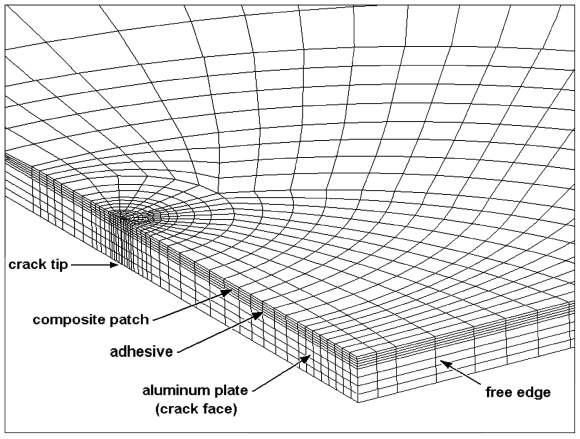

Fig. 9 Three-dimensional view of the cracked region.

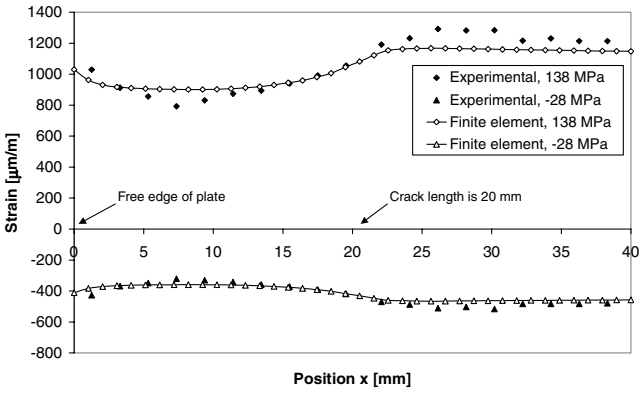

Fig. 10 Longitudinal strain distribution in undamaged repair.

is offset from the surface of the repair by a small but not insignificant distance that tends to amplify bending effects. The experimental strains are reported as the average strain for gauges mounted on the patches on either side of the specimen, and results are shown for an applied tensile stress of 138 MPa and a compressive stress of −55 MPa. In this case, the crack was 19.9 mm long.

The strains determined for the outer surface of the patch are lowest in the region of the crack in both the model and experiments. The load should largely be diverted to the patch as it bridges the crack, thus increasing the strain. The cause for reduced surface strains in this region is induced bending due to the neutral axis offset caused by the crack and the overlying patch. This is evident in the through-thickness stress gradients observed in the finite element model. Even with the honeycomb support, under tensile loads the structure experienced bending sufficient to noticeably reduce the strains on the outer surface of the patch.

After 175,000 cycles, the crack was nearly 45 mm long, and the interface between the patch and underlying cracked plate had a disbond of approximately 5-mm length. Figure 11 shows the adhesive-layer mesh and is provided to show the modeling of the disbond. The gray elements were removed to impose the disbonded condition observed in the fatigue experiment.

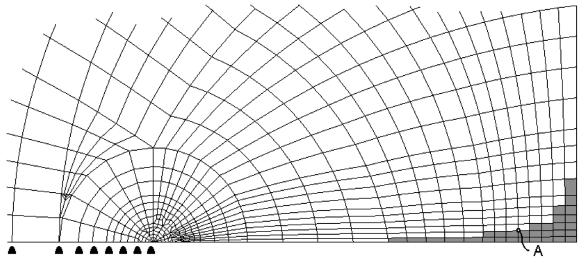

Fig. 11 Adhesive elements in the region of the crack, showing the disbond.

Similar to Fig. 10, Fig. 12 shows the surface strains in the patch as it reinforces the cracked plate. It is unfortunate that the strain gauges did not extend far enough to measure the strains at the crack tip, but much can still be made of the results. For both the finite element model and the actual specimen, the strains reach a peak at the free edge of the patch. A traditional center-cracked repair model would predict a maximum strain at this location, but it should be reached gradually. There are two likely reasons for this abrupt peak: 1) the edge-cracked geometry of the plate has a significantly lower stiffness than a center-cracked plate at this location and hence it will shed more

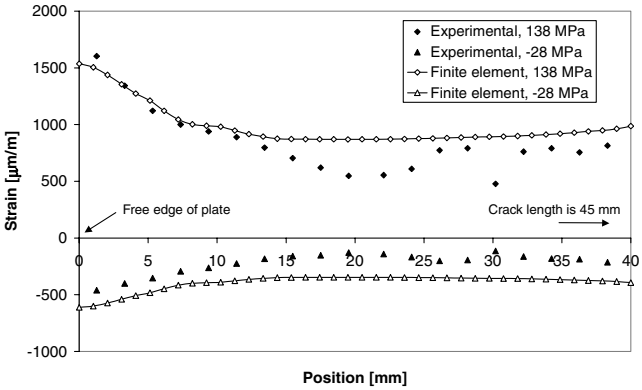

Fig. 12 Strain distribution, with honeycomb.

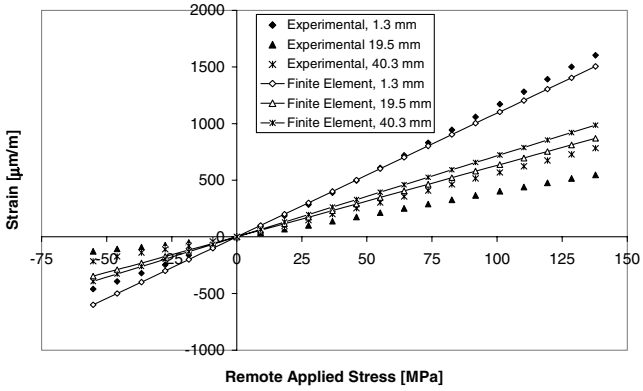

Fig. 13 Variation of strains with applied stress, with honeycomb.

load to the patch and 2) the disbonded part of the patch has a low bending stiffness and will tend to shed the bending loads to other areas, an effect that increases when the honeycomb core is removed. The increase in load at the edge of the patch and adhesive edge effects also leads to larger adhesive stresses and a faster rate of disbonding near the free edge.

Figure 13 shows the surface strains measured by selected gauges plotted against the remote applied stress. The gauges are shown at selected distances from the free edge of the repair. The strains are linear until the applied stress is well into the compressive region, when tensile residual stresses in the substrate are overcome and crack closure reduces the proportion of the load carried by the repair. The distances in the legend are the position of the strain gauges, (i.e., x in Fig. 8b). The finite element results are from a linear model and do not include crack closure, which is seen to reduce the compressive strains observed in the experimental results when compared with the strains measured under tensile loading.

The next stage of testing occurred after the removal of the honeycomb core separating the aluminum plates. The specimen

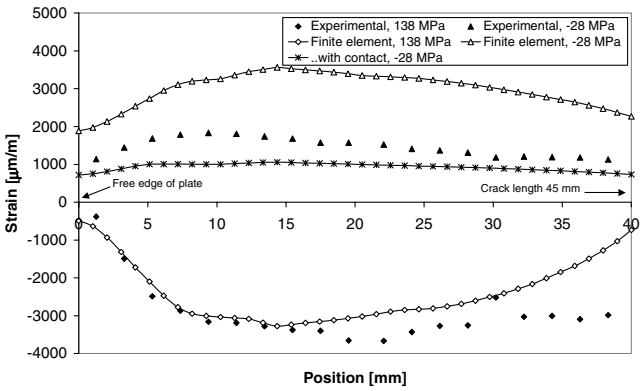

Fig. 14 Strains, without honeycomb.

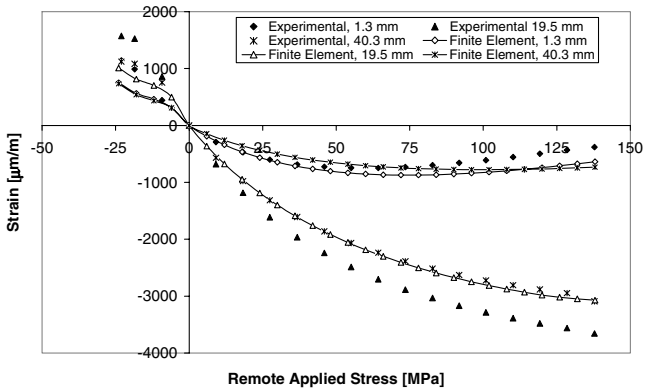

Fig. 15 Variation of strain with applied stress, without honeycomb.

experienced no further fatigue cycling at this point, and so the crack and disbond sizes are the same as for the previous case. Figure 14 again plots the strain distribution on the surface of the repair. Note that applied tension results in compressive strains on the surface of the patch. The honeycomb provided a large degree of constraint against bending, and now that it has been removed, bending stresses dominate the response of the repair. This bending and the resulting adhesive peel stresses must be accounted for to predict the rate at which a repair will fail. After removal of the honeycomb, the maximum applied compressive stress was only −28 MPa, and the patch appeared to be approaching collapse. Here, the effect of the edge-cracked-plate geometry combined with the reduced bending stiffness of the disbonded section of the patch is again evident in the dramatically increasing strains near the edge of the patch. It can be seen that crack closure plays a significant role for compressive loading for both the finite element model results and the measured strains, and hence crack-face contact should be included to obtain accurate results under compressive loading.

In Fig. 15, selected strain results are plotted against applied load. The strains are clearly nonlinear without the honeycomb support and show good agreement except at 40.3 mm, the strain gauge nearest to the crack tip. This discrepancy is likely due to a small amount of disbonding near the crack tip or adhesive plasticity, neither of which was included in the finite element model. Both of these effects would act to relieve the severity of bending of the composite patch as it bridges the crack. The compression results again show the importance of crack closure, which acts to unload the patch near the crack.

The finite element model and experimental results capture the geometrically nonlinear mechanical response of the bending repair and demonstrate the importance of bending on the stresses within the patch itself. The importance of modeling the finite geometry of the edge-cracked plate has also been demonstrated, because a significant peak in the patch strains was observed at the edge of the repair. Crack closure was also shown to have a large role under compressive loading, acting to greatly relieve the load carried by the patch. This beneficial effect, however, is offset by the potential for elastic buckling, which appeared to be imminent for the unsupported repair under an applied compressive stress of only −28 MPa. In the next section, this validated finite element model will be used to calculate the residual strength of the repair and to examine factors affecting its fracture strength and fatigue life.

V. Residual Strength and Damage-Tolerance Assessment

The fractographic examination illustrates the failure mechanisms at work in the repair. One important observation is that crack growth and disbond growth appear to occur together, which should be expected, because crack growth in the aluminum plate will generally shed load to the patch and promote disbonding. Similarly, disbond or delamination growth will reduce the effective stiffness of the patch as it bridges the crack and promote further cracking in the aluminum. The final failure of the structure occurred by simultaneous fracture of

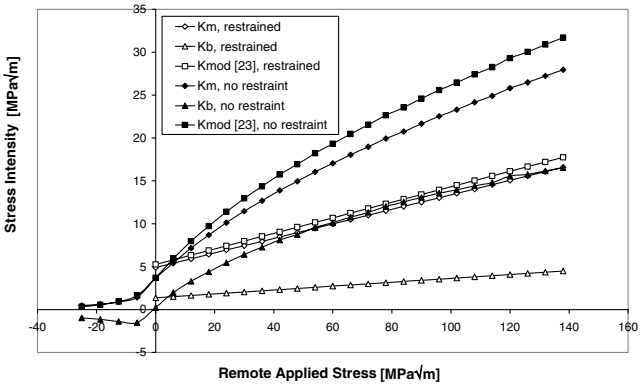

Fig. 16 Membrane and bending stress-intensity factors.

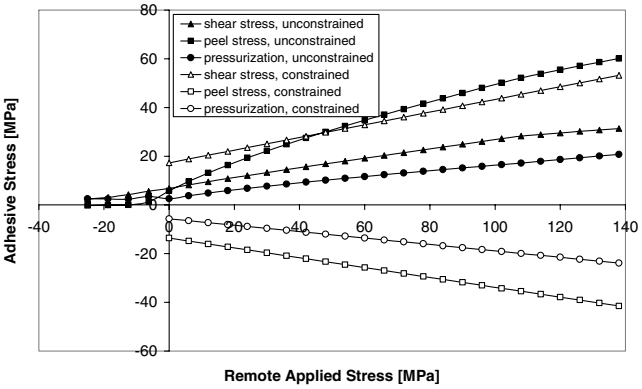

Fig. 17 Adhesive stresses.

the composite patch and the repaired plate. Another important observation is that composite delamination and composite fracture are significant failure modes when a repair is free to bend, neither of which are often observed in double-sided repairs or repairs with bending restraint. It is clear that to assess the strength of a one-sided repair, full account must be made of the potential for failure in three areas: 1) cracking in the aluminum substrate, 2) failure of the adhesive, and 3) failure of the composite. The following sections address these three areas of concern and place into perspective the relative merits of both existing and proposed methods of evaluation (resulting from the current investigations) for the purposes of damage-tolerant design of bonded composite repairs on metallic structures.

A. Aluminum Substrate Fracture

Figure 16 shows K_m and K_b as predicted by the finite element model for two cases: with and without the honeycomb bending restraint. The predicted results reflect the previous experimentally observed nonlinear deformations, with stress stiffening acting to reduce the rate of increase in stress intensity under larger applied loads. This happens when the structure moves toward the load line and sheds load to regions remote from the crack.

By linear elastic fracture mechanics (LEFM) criteria, fracture is considered imminent when the sum of K_m and K_b exceeds the plane-strain fracture toughness K_{1c}. For thin aircraft skins, the actual fracture toughness (denoted as K_c) is often used. K_c is usually obtained from testing and because it is often significantly greater than K_{1c}, it will result in a longer critical crack length and thus can greatly ease inspection requirements. The increasing acceptance of the NASGRO [23] damage-tolerance software package allows the use of a calculated K_c in most circumstances, but caution is required for short cracks, for which the nonsingular stresses near the crack tip are significant. For the 2024-T3 plate used in this investigation, $K_{1c} = 34\ \text{MPa}\sqrt{m}$ [22], whereas for a 3.175-mm-thick 2024-T3 plate, NASGRO provides a K_c value that is over twice as large. For the AMRL specimen with a crack size of 45 mm, K_{1c} is exceeded, with an applied remote stress of nearly 90 MPa for unrestrained bending, but requires well over 140 MPa to exceed K_{1c} with the honeycomb bending restraint present.

Fatigue is also well characterized by the stress intensity, with crack growth properties being catalogued in well-accepted software tools such as NASGRO or AFCRACK. Difficulties can arise due to load interaction and crack closure, load spectrum, adverse environments, and plasticity or thickness effects, often requiring the use of experiments to evaluate crack growth under realistic conditions. Duong and Wang ([24], Eq. 5) characterized crack growth under combined bending and extension using a modified stress intensity K, which demonstrates good results when compared with test data for AL7075 specimens. K is developed by interpolation between two states for which crack growth can be accurately assessed: 1) a crack experiencing only a membrane stress intensity, and 2) a crack with equal membrane and bending stress intensities. From Fig. 16 it can be seen that there is a significant increase in K after removal of the honeycomb. Given that as little as a 15% increase in ΔK can halve the fatigue life, it is apparent that bending has a large role.

B. Adhesive Failure

Adhesive failure is dependent on the adhesive stress or strain state that develops as the repair acts to bridge the crack. Figure 17 shows the peak shear and peel stresses at the edge of the crack for location A in Fig. 11. The results exhibit nonlinear behavior, with the adhesive stresses for the unconstrained case nearly vanishing under a compressive remote applied stress, in which the crack will close as the thermal residual strains are overcome. These results include thermal residual strains in the adhesive as well as in both the patch and plate. This was accomplished using an effective stress-free temperature of 81°C [7]. It must be noted that in the finite element model, the peel and pressurization (i.e., hydrostatic) stresses vary significantly through the thickness of the adhesive, an observation that other researchers have also observed in bonded joint models. It was not possible to examine this effect in detail with this finite element model because of size restrictions on the university version of ANSYS. Similarly, finite element results for the adhesive compression in the unrestrained case are likely to be over-reported because no attempt was made to model crack closure between the surfaces of the adhesive disbond. Closure of the adhesive crack faces would relieve a portion of the compressive adhesive stresses in the restrained specimen. It must be noted that the adhesive is modeled using linear elastic constitutive properties even though localized yielding would be expected, particularly under hot and wet conditions.

Adhesive strength depends on whether yielding or fracture is prevalent. In hot and wet conditions, high temperatures and the plasticizing effect of absorbed water act to make yielding dominant. At low temperatures associated with high altitude, fracture becomes prevalent. The main design criterion is the adhesive stress, which should be kept low to ensure that fatigue failures will not initiate and gross yielding will not occur under limit loads. Shear and peel stresses are controlled using an appropriate adhesive thickness, providing long overlap lengths to minimize bending loads and peel stresses, and by tapering the edges of the joint. The strength of the Cytec FM73M adhesive under various degrees of constraint and for laboratory or hot and wet environmental conditions is well characterized by the work of Chalkley and van den Berg [25], Ignjatovic et al. [26], and Wang and Chalkley [27]. The failure surface for this adhesive is pressure-dependent and is best characterized by the Drucker–Prager cap plasticity model [26], particularly in the presence of compressive pressurization. It can be seen in Fig. 17 that compression of the adhesive is not a concern for unbalanced repairs (the no-constraint case), because the crack faces will close and the aluminum will carry the stresses, unloading the adhesive. The authors use a simpler model, based on [25,26], whereby the adhesive will obey the Tresca or von Mises criterion under compression and the modified Tresca or modified von Mises criterion under tensile pressures, thus providing the limit shear yield strength, as defined next.

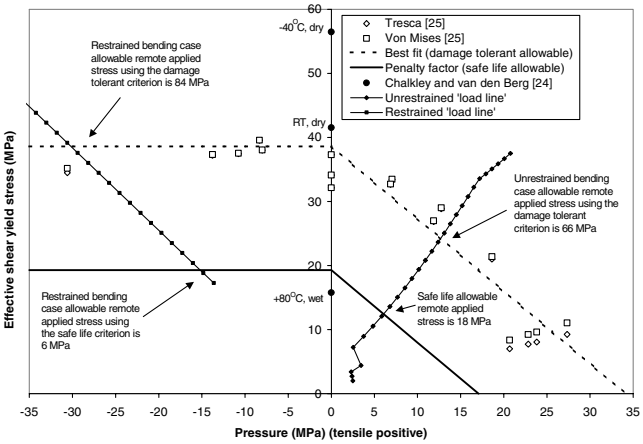

Fig. 18 Adhesive yield criteria and finite element model adhesive stresses.

$$\tau_y = \begin{cases} 38.6 \text{ MPa} & p < 0 \text{ MPa} \\ 38.6 \text{ MPa} - 1.13p & p \geq 0 \text{ MPa} \end{cases}$$

This best-fit criterion is plotted in Fig. 18, along with a criterion that has been developed to account for environmental effects, and employs a penalty factor of 2 against both the shear and pressurization stresses, as suggested by Chalkley and Baker [21] for the shear stress allowable. Note that Royal Australian Air Force (RAAF) design guidelines allow adhesive loading to 80% of the allowable shear strain [28]. For comparison, allowable shear stress results from Chalkley and van den Berg [25] are shown in Fig. 18 for various environmental conditions.

The trace or load line of the finite element model adhesive pressurization and shear stresses is plotted in Fig. 18 for both the restrained bending and unrestrained bending cases. For restrained and unrestrained bending, the adhesive should begin to yield under remote applied stresses of 84 and 66 MPa, respectively. It is apparent that the adhesive was repeatedly loaded into the plastic range during the fatigue testing and that without bending restraint, significant peel stresses and pressurization developed in the adhesive near the crack, explaining the rapid failure of the repair. Applying the safe-life design criterion that includes factors to account for environmental effects, neither of the two cases would result in a useful load-carrying capability. It is clear that the safe-life allowable stress is very conservative and would be difficult to meet in the presence of a long crack under a repair. It is an appropriate criterion, however, in the tapered region, in which good design can reduce the adhesive stresses. In the region near the crack, environmental concerns are less likely to be critical, and the damage-tolerant allowable may be more suitable, perhaps with a reduction such as the 80% of allowable shear strain policy used by the RAAF.

One must also assess adhesive fracture and fatigue. Because adhesive strength and stiffness result from molecular and intermolecular forces that exhibit strain rate, moisture, and temperature sensitivity, damage-tolerance substantiation must include both the detrimental effect of cold temperature on fracture toughness [29] and the effect of high temperatures that induce plasticity and accelerate fatigue crack growth. The use of energy-based fracture parameters is complicated by the dependence of the stress distribution on the joint loading type, geometry, and material composition. This violates the similarity criterion, whereby it is assumed that cracks have similarly shaped stress distributions regardless of crack length, position, or geometry and thus explains why inconsistent results can arise when they are used to predict fracture and fatigue [8,30]. A final complication is that either of two modes of cracking may occur: cohesive and adhesive. Cohesive failures occur when the adhesive fails by yielding and cracking, whereas adhesive failures occur at the bond line. There is debate over whether pure interfacial failure can occur or if it occurs by low-energy fracture of the weaker material due to constraint from the stiffer and (usually) stronger material present. But it is generally agreed that for a well-designed joint, adhesive failures should not occur unless a bond surface has been poorly prepared (i.e., the principle forming the basis for quality assurance testing of bonded joints). These are significant challenges and, in practice, test data from specimens with a similar composition, geometry, and loading are required. Many researchers in the bonded composite repair field have been critical of the strain-energy-release-rate approach to adhesive fatigue and fracture, and other options have been suggested including use of the Hart-Smith [31] plastic strain energy density or plastic strain range [8] approaches. In spite of this criticism, the use of strain energy release rates for specific geometries and loading conditions has provided some excellent results [32–39], and a body of literature exists for the Textron 2251 boron prepreg and Cytec FM73M patch system (e.g., [40–42]), which includes information on fatigue threshold and environmental effects.

Here, the authors test the use of elastic adhesive stresses as a conservative criterion for fracture and fatigue assessment of the adhesive. In a previous round-robin test of bonded joint analysis methodologies for the cracked lap-shear specimen [43], Joseph and Erdogan demonstrated that the opening and shear-mode strain energy release rates are related to the peak peel and shear adhesive stresses. This approach builds on the strain-energy-release-rate arguments of Rice [44], an approach that is considered to provide exact results for many fracture problems and that has been applied by other researchers (e.g., [8,45]). The round-robin testing showed that this method of strain-energy-release-rate calculation provides reasonable results when compared with other techniques such as modified crack closure. Accordingly, the opening- and sliding-mode strain energy release rates may be calculated from the peel and shear adhesive stresses as follows:

$$G_{\mathrm{I}} = \frac{t_a \sigma_p^2}{E_a}, \qquad G_{\mathrm{II}} = \frac{t_a \tau_p^2}{G_a}$$

For a linear elastic homogeneous material, the strain energy release rate may be converted to a stress intensity using the plane-strain relationship $K^2 = GE_a/(1 - \nu_a^2)$. Thus, the adhesive stresses G and K should be more or less equally capable of predicting fatigue and fracture in the elastic regime for joints of similar composition and loading. In the plastic regime, the elastic–plastic strain energy release rate J can be calculated by defining contours outside of the crack-tip process zone and using energy arguments to determine the rate of work. J is effectively independent of the state of the process zone unless the plastic strains are sufficient to cause significant changes in the energy state of the elastic region of the specimen. In this case, the method of Erdogan and Joseph will still provide accurate results and the adhesive stresses G (or J) and K based on an elastic analysis are still more or less equally capable of predicting fatigue and fracture. Similar to the method of Erdogan and Joseph, the strain energy density and adhesive stresses are also simply related for a linear elastic material. Accordingly, although each of these various measures of the state of the adhesive has advantages concerning how it is calculated or assessed from a numerical model or experimental results (and some provide a better representation for an adhesive experiencing creep or gross plasticity), there is, in many ways, little to choose from between them, particularly when one considers that the design criteria will essentially restrict the thickness-averaged adhesive stresses to the elastic range. The main difference is convention, whereby an analyst will understand a critical stress intensity to imply a material property, whereas a strain energy release rate should be understood as a measure of the energy absorbed during the failure of a particular specimen under particular conditions. For repair and overhaul, there is not the time, information, or expertise to perform sophisticated analysis, and even with conventional repairs, simple and conservative means are often preferred, even at the expense of increased operational burdens such as higher inspection frequency or early scrapping or rework. Accordingly, the authors will use the available experimental data to test the stress-based adhesive failure criteria.

As a comparison of adhesive failure criteria, Fig. 19 plots experimental data from several sources against the yield criteria by

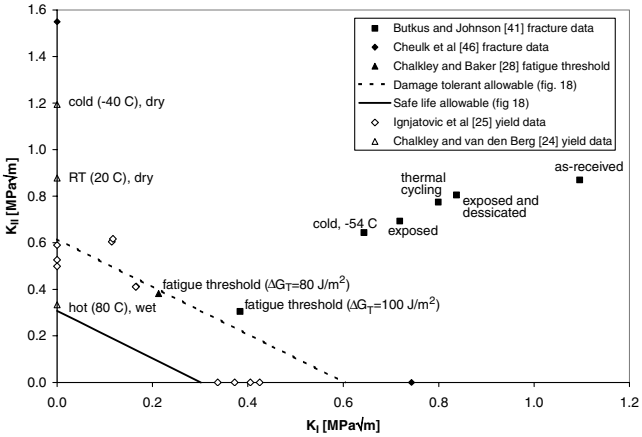

Fig. 19 Comparison of adhesive fracture data and yield criteria.

assuming an adhesive thickness of 0.17 mm, which is the value used by Butkus and Johnson [41]. The data were converted from adhesive stresses and strain energy release rates to opening-mode K_I and sliding-mode K_{II} stress intensities, as described earlier. Given the complex interactions between the boron fibers, matrix, and adhesive, this conversion does not imply that the actual stress intensity at the tip of a crack has been calculated. The plotted results indicate that the stress-based criteria are conservative in all cases, even when including environmental effects and matrix or interface cracking. It is also seen that for this adhesive thickness, the yield criterion and room-temperature fatigue threshold (including environmental effects) are similar and a criterion based upon the adhesive stresses should be adequate for both fracture and fatigue. Note that Butkus and Johnson used a threshold of 10^{-9} m/cycle, whereas Chalkley and Baker [21] used 6×10^{-9} m/cycle.

For fatigue assessment, it has been proposed by many (e.g., [8,32,38]) that the adhesive stresses be low enough that disbond growth will not occur. Hart-Smith [46] also emphasized that well-designed bonded joints should be designed for an infinite life and that the locus of failure or weak link in the structure should not be the bond. This proposition arises because adhesive joints exhibit high disbond growth rates that increase very quickly with an increase in the applied fatigue load and because through good design it is usually possible to reduce the adhesive stresses to the point at which fatigue cracking is extremely unlikely. It is suggested that the unmodified adhesive failure criteria be employed in the damage-tolerant region about the repaired crack and that the safe-life criteria (to account for environmental effects) be used for the safe-life region about the edges of the repair. This is in accordance with the definition of the safe life and damage-tolerant regions of a repair as defined by Baker [60], but to some degree this runs counter to the advice of Chalkley et al. [8], who suggested that a stress-based approach for fatigue assessment may not be appropriate because in their experiments, the specimens with the highest stresses were not always the ones that failed first. However, given the experimental threshold data shown in Fig. 19, which by nature accounts for the effects of local stress raisers (e.g., due to fiber geometry and layout, adhesive imperfection, etc.) that are not included in most repair models, it should be adequate to simply show that limit loads do not result in adhesive stresses that exceed these allowables. This is particularly true if one considers that the effective once-per-flight fatigue loads (the load that would be applied once per flight cycle to represent all the fatigue damage accrued by the actual fatigue spectrum) are typically well below limit load (usually below 60% of limit load) and that the fatigue threshold data applied are typically for room-temperature testing, whereas flight loads will tend to occur at high altitude, at which the lower temperatures enhance fatigue strength. Accordingly, the authors suggest that a stress-based approach, although imperfect, would still be applicable by the principle of compounded conservatism ([48], Sec 9.5). Compounded conservatism is the practice of applying many "worst-case" conservative assumptions together to ensure safety, and although it may lead to an inefficient design, it does ensure safety in the face of a number of factors that are difficult to quantify (e.g., temperature and environmental effects, fatigue that may be dominated by very local structural details, or stochastic variations in properties or material processes).

C. Composite Fracture and Delamination

The textbook approach to composite failure analysis is to use interactive failure criteria such as the Tsai–Wu theory (e.g., [49]). These theories extend the energy-based failure criteria that have been successful for homogeneous anisotropic ductile solids to the analysis of heterogeneous fiber-polymer composites that exhibit fracture-dominated failure modes. Pioneering data on the application of the Tsai–Wu failure theory are available for boron fibers with an older matrix system [50,51]. The other general class of failure criteria arises from mechanistic modeling, in which individual failure modes are analyzed to form a set of equations that form a failure envelope based upon stresses or strains. The worldwide failure exercise [52] tested several composite failure criteria against a set of tests that are representative of design problems arising in different industries. Interactive theories were found to give good results in most cases, but caution was urged in their application to unidirectional lamina, for which unconservative results could be obtained. Most criteria provided reasonable results for the types of problems for which they were designed, including maximum stress or strain criteria that are often used for specific applications in codes and standards. It was emphasized that careful interpretation of the results is required and that for large deformations or final failure strength, nonlinearity and progressive damage are important considerations. Recognizing that for a limited-size repair patch, weight optimization is not critical, then a simple patch design criterion becomes preferable and adequate when supported by experimental data, and a mechanistic approach expressed in terms of simple stress or strain limits may be appropriate.

Hart-Smith [53] made a convincing case that the various constituents and failure modes of the composite should be treated separately and that interaction should be handled by superposition of loads, allowing the strength of the composite to be assessed through separate analysis of the constituents (fibers, matrix, and interface) under the combined loads (including cure-induced thermal residual stresses in the matrix), leading to a failure envelope composed of several individual criteria for each constituent. Micromechanical failure models are often only required for the development of engineering design allowables, and resulting individual failure criteria are often quite simple. Hart-Smith catalogued the typical failure mechanisms, which (after elimination of those that are not relevant to crack-patching with a unidirectional patch) are summarized as follows: fiber fracture due to fiber or composite discontinuities and fiber failure under tensile loads, fiber microinstability and fiber shear failure under compressive loads, ductile matrix failure under in-plane loads, matrix cracking under transverse-tension (geometry-dependent), interfacial failure between fiber and matrix, interlaminar failure at edges and discontinuities, and delamination under impact or transverse shear loads.

Within Federal Aviation Administration guidance documents and the crack-patching literature, it has been stressed that composite and adhesive failure modes must be addressed. Because the technology has been used primarily in structures with significant bending restraint and primarily tensile loads, composite failure mechanisms other than progressive adhesive disbonding or delamination have rarely been observed. The requirement for fatigue test validation has also provided a definitive control on composite failure modes. With increasing interest in the use of single-sided repairs and wider application of generic repairs without specific tests, it will be necessary to specifically address each composite failure mode, especially considering that single-sided repairs are much more susceptible to composite failures and instability under compressive loads, as demonstrated by the testing carried out by the authors, as described earlier.

Given that 1) for most boron/epoxy repairs the primary load path is in the primary direction of the patch, 2) the aluminum substrate will

support out-of-plane loads, 3) crack closure will shield the composite patch from the worst of the compressive stresses, and 4) the tensile strength of the boron patch is high compared with the underlying aluminum plate, it should generally not be necessary to perform a sophisticated analysis of the many possible failure modes to assess the strength of the composite patch. The margins against both matrix and fiber failure should generally be high, except in the presence of significant bending and peel stresses, which may promote matrix cracking (due to transverse stresses) and the failure of fibers on the inner or outer surface of the repair. Transverse loading can result in matrix or interfacial failure as stiff fibers lead to stress concentrations in the matrix, causing it to fail before the nominal transverse stress exceeds the strength of the matrix. From testing and fractography, it has been shown that the exact geometrical distribution of the fibers has a significant role, and a strength reduction factor must be used to develop a failure criterion for the composite [49]. It is suggested that the adhesive-stress allowables already cover this assessment of the composite matrix, including the temperature and environmental effects and the stress concentrations in the matrix due to the constraint of the fibers. The adhesive stresses are representative of the critical matrix transverse stresses and the Butkus and Johnson [41] data provide assurance that they will be held to an appropriate level.

Under axial loads for a unidirectional polymer-reinforced composite such as boron/epoxy, failure occurs when the stress in the boron fibers reaches its maximum, corresponding to a nominal tensile stress in the orthotropic solid. This is the principal strength of the composite, and Textron product data [20] specifies a tensile strength of 1520 MPa at room temperature and 1450 MPa at elevated temperatures. Fatigue under such loading may be characterized by a stress-life (S-N) diagram, with small reductions in stiffness and strength occurring as the matrix cracks and delaminates near fiber breaks and stress concentrations. When compressive stresses occur (possibly due to bending), transverse stresses and interlaminar failure have a detrimental effect. Tensile interlaminar stresses develop due to the buckling of fibers, and transverse stresses may cause interlaminar failure. This form of fiber-buckling is controlled by the adhesive shear yield stress [49]. Textron product data provide a compressive strength of 2930 MPa at room temperature and a much lower 1250 MPa at elevated temperatures. Because the compressive strength is largely controlled by the matrix shear strength, it is suggested that the lower value be used as a basis for a conservative design allowable.

In the experimental work described earlier, the composite repair was observed to have failed via partial delamination and, ultimately, by fracture under combined bending and axial loads at the edge of the disbonded region. The composite-laminate stresses at point A of the finite element model are presented in Fig. 20, in which it can be seen that the sum of the membrane and bending stresses in the composite laminate is high but does not exceed the principal strength of the composite (as quoted in the preceding paragraph) for either restrained or unrestrained bending. Fiber failures were observed in the experiments, occurring near the adhesive/patch interface, and could be explained by either fatigue failure under the relatively high composite-laminate stresses or by the action of adhesive/matrix peel stresses on loose fibers. These adhesive/matrix peel stresses (shown in Fig. 17) are high after removal of the bending restraint and could act to break individual fibers that come free of the matrix due to delamination.

Although comparison with the results of this single test is not definitive, it is likely that the principal strength design criteria are adequate for the composite patch itself, as long as the adhesive-stress design criteria are adequate to rule out early failure due to transverse stresses. This can be confidently stated because the strength of the boron/epoxy patch is very high relative to the substrate. It may prove to be necessary, however, to develop a knockdown factor to account for fatigue (i.e., to keep the stresses low enough to prevent composite fatigue failures during the life of a patch), but there should generally be a sufficient margin to cover such a strength reduction.

Given that the adhesive design criteria adequately cover the possibility of early failure due to high transverse normal or shear stresses in the matrix and that the composite strength accounts for

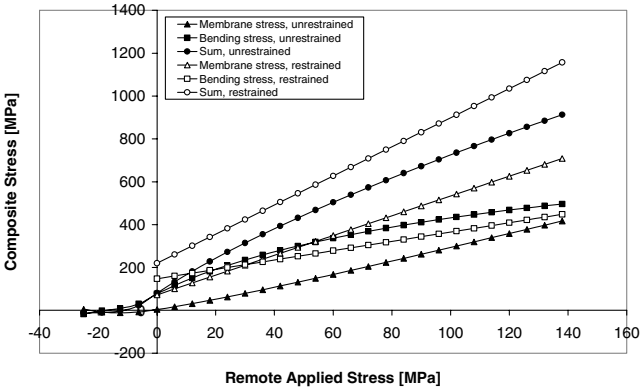

Fig. 20 Composite stresses.

failure from tensile or compressive stresses, early patch failure should only be possible due to impact damage or significant composite discontinuities such as twisted, irregular, or damaged fibers. Currently, low-velocity impact tests are required to determine the susceptibility of a repair to such conditions. Because "best practices" and the proposed adhesive and composite design criteria will keep the stresses low in the bulk of the repair through good design, only low rates of subcritical damage growth should occur in the event of such discontinuities. One would not expect significant growth of interply or impact damage unless it is accompanied by fiber damage or occurs in a region experiencing significant bending and through-thickness stresses, compressive loads, or very large transfers of load through shear (such as might exist near a repaired crack or about the edges of the patch). In practice, this has proven to be true, with experimental results suggesting that delamination growth from impact damage or manufacturing-related discontinuities away from load transfer regions is minimal [11]. Accordingly, damage growth should only occur in highly loaded regions, such as about the crack and near the edges of the repair, in which the stresses have already been controlled through the proposed design criteria.

D. Synergy of Aluminum and Composite/Adhesive Fracture Criteria

The final failure of the patch observed in the experimental investigation was via simultaneous fracture of the repair and plate due to the overload of the composite by local bending and axial loads at the edge of the disbond. For symmetric repairs or repairs with significant bending restraint, failure has been observed to occur by fracture of the repaired plate and simultaneous growth of an adhesive disbond through to the edge of the repair, typically with the composite patch itself otherwise being undamaged. It is possible to model either scenario using a detailed finite element analysis using nodal release and element removal to model the growing crack and disbond or by generating a new model for every increment in crack growth or disbond growth. The actual residual strength can then be determined by whatever ratio of cracking and disbonding led to a natural balance between the failure of the patch and the repair/adhesive (e.g., [54]). Simplified finite element techniques (e.g., [12,13]), boundary element models (e.g., [10]), and crack-bridging models [55] have all been used to evaluate the life of a repair with a growing disbond and crack. The authors have recently developed a new crack-bridging model for coupled bending and extension [56] and geometrically nonlinear coupled bending and extension [57], which should allow for rapid assessment of unbalanced repairs.

The concept of synergy between crack and disbond growth and a natural disbond size, when combined with the allowable-stress criteria described earlier and effective models for combined crack and disbond growth, leads to a new opportunity to simplify the damage-tolerance substantiation of a repair. Experience suggests that limited disbonding will often occur near a repaired crack in a highly loaded structure and that additional analysis will be required to fulfill substantiation requirements and ensure that the patch is sufficiently large to provide adequate damage tolerance against disbonding. It is

suggested that in the absence of a fatigue test that demonstrates otherwise, one must assume that the adhesive has debonded about the repaired crack to the point at which the adhesive stresses drop to a threshold value (i.e., the damage-tolerant allowable). This will, in effect, result in disbond growth that is controlled by growth of the repaired crack under fatigue loading, in which both the crack and disbond size are determined by applying standard LEFM techniques to the crack alone, using the as-reinforced stress intensity (i.e., K_{mod}, as calculated earlier). Because crack growth in the metal substrate is well-characterized, the issue of fatigue crack growth rate prediction for the adhesive is avoided, allowing a rational determination of the inspection criteria.

VI. Discussion

The experiments and the validated finite element analysis demonstrate the potential for early failure of a single-sided bonded composite repair due to induced bending. The tested geometry was initially designed to include bending restraint and did not have a sufficient overlap length to minimize bending loads and adhesive peel stresses. Without bending restraint, failure occurred very rapidly, illustrating the need for adherence to bonded joint design guidelines, particularly the use of sufficient overlap lengths. The observed failure modes included rapid disbonding of the adhesive at the adhesive-composite interface, fiber breaking, and, ultimately, simultaneous failure of both the repair and the underlying plate. It was shown that nonlinear analysis techniques are required for the accurate analysis of a repair and that crack-face contact must be modeled to evaluate a repair under compressive loads. These results show that composite and adhesive failure modes must be treated very seriously for single-sided repairs, and the specimen proves to be an extreme test for patch design methods.

In the second half of the paper, finite element results for the stress intensity in the underlying plate, the stresses in the adhesive layer, and the composite patch stresses were compared with failure criteria for fatigue, yielding, and fracture. It was shown that the underlying plate can be treated using LEFM and that adhesive and composite stresses can be controlled to ensure integrity of the patch. Linear elastic analysis is used to determine the adhesive stresses and a failure criterion, and a method for fatigue assessment is proposed that accounts for adhesive pressurization and places a large penalty on peel stresses. Most of the complications of fatigue and fracture assessment of bonded joints are encapsulated within the proposed allowable stresses, allowing for a relatively simple assessment of the joint. With more experimental work to justify the design allowables and with appropriate closed-form tools for repair analysis, most repairs should be able to be certified using a simple analysis of this type.

The principal strength of the composite was also shown to be an adequate criterion for longitudinal tensile loads in the unidirectional patch. Because the compressive strength of the composite is determined primarily by the shear strength of the matrix, the authors suggest that the high-temperature compressive strength be used as the allowable stress in compression. This corresponds to the approach developed by the authors for evaluation of the adhesive and of the composite matrix under transverse loads, whereby it was shown that a simple stress-based criterion is generally adequate for damage-tolerance substantiation of a repair.

The stress-based adhesive failure criteria were achieved by directly comparing the adhesive yield criteria to fracture criteria via Joseph and Erdogan's definition of the strain energy release rate for a bonded joint. The technique is promising but needs further investigation to validate. Specifically, the adhesive yield criteria under combined peel and shear stresses need to be established under hot and wet conditions, and more fracture strength and fatigue threshold data need to be generated for the aluminum/FM73M/boron/epoxy system, considering the effects of adhesive thickness and environment. This would entail a detailed testing program, but would establish an authoritative stress-based design allowable for bonded repairs. Because the practical working range of an adhesive in this application is only 0.125 to 0.250 mm [58], the scope of this additional testing should not be overly expensive or onerous. An additional problem that needs to be addressed is that to ensure consistency in the comparison of the test results, Joseph and Erdogan's method should be used throughout. It is noted that the strain energy release rates reported by Butkus and Johnson [41] were calculated using the virtual crack closure technique. Finally, the criteria should be tested against the working stresses in the many repairs that were accepted for certification through a comprehensive damage-tolerance substantiation process, to ensure that the proposed stress-based design criteria are sufficiently conservative when compared with established practice. The observation that the composite patch and the repaired plate fail in a synergistic manner, when combined with the simple stress-based design criteria that encapsulate the many complex damage mechanisms that can occur within a repair, leads to a new opportunity to evaluate the design life of a repair and the ability to assign an inspection interval without a detailed analysis of the fatigue response of the adhesive. In this proposed approach it should be assumed that an adhesive disbond will exist that is large enough to reduce the adhesive stresses to the threshold level. The fatigue assessment and damage-tolerance substantiation can then be can carried out based on the crack length alone, with the ultrasonic or thermographic inspection of the repair being carried out at the same time as the eddy-current inspection of the underlying crack.

Based upon the adhesive-stress design criteria and the residual strength and fatigue life of the unrepaired crack, it is possible to divide repairs into four categories, as shown in Fig. 21. By applying the principle of compounded conservatism and by applying a simple risk assessment to ensure that the safety of the repaired structure is higher than that established during the design of the original damage-tolerant structure, it is possible to develop acceptance criteria for bonded repairs applied to weakened or damaged structures.

Repair designs in quadrant A have very low working stresses in the composite/adhesive and the underlying structure has adequate residual strength even without the repair. In practice, the working stresses in many transport airframe components are low and the structure can tolerate very long (e.g., bay-to-bay) cracks and still survive limit load due to other reinforcing structures such as stringers and frames. Under this scenario, for the repair of a relatively short crack, the authors suggest that the repair may be substantiated without much further work, with inspections based on the crack growth predicted in the equivalent unrepaired structure. The only additional work required would be to ensure that load attraction to the patch does not result in early failure in regions about the edge of the repair or in surrounding structures.

In quadrant B, the adhesive stresses are locally high, but the patch is not really required to establish inspection criteria for the underlying structure, because it has sufficient residual strength. This could occur in the event of a very small crack, an accidental hole, an underdesigned structure, or a corrosion grind-out in an area in which,

Quadrant A	**Quadrant B**
adhesive and composite qualifiable by compounded conservatism, using allowable stresses and adequate residual strength in unrepaired original structure	adhesive and composite not qualifiable by compounded conservatism (e.g. allowable stresses exceeded near a crack) and adequate residual strength in unrepaired structure
Quadrant C	**Quadrant D**
adhesive and composite qualifiable by compounded conservatism and inadequate residual strength in unrepaired original structure (e.g. there is a long crack or a significant corrosion grind-out)	adhesive and composite not qualifiable by compounded conservatism and inadequate residual strength in original structure

Fig. 21 Proposed classification of repairs by damage-tolerance substantiation requirements.

due to geometric constraints, it is not possible to reduce the stresses in the composite/adhesive sufficiently to meet the very stringent design criteria or for a reinforcement used to strengthen an underdesigned but undamaged structure with high working stresses. Here, the adhesive/composite interface is likely to fail in a progressive manner, which could be addressed by reexamining the limit loads to see if they are due to flight or landing loads (i.e., a fatigue case such as a vertical gust) or whether hot and wet conditions are likely to exist during the limit-load maneuver. In the event that such a reevaluation of the loads is insufficient, then a damage-mechanics analysis of the patch or a static test may be required to demonstrate that the patch itself will have sufficient strength even in a highly damaged state.

Like in quadrant A, repairs in quadrant C have low working stresses, but the underlying structure has significant damage and the reinforcing effect of the patch is required. An example might be a large fatigue crack emanating from a stress concentration in an otherwise lightly stressed fuselage panel. Here, the primary concern is the possibility of an unpredictable early failure of the repair due to poor surface treatment of the aluminum surface for bonding. Quality assurance and bonding procedures minimize the probability of this type of failure, but cannot eliminate it, particularly for one-off repairs applied in the field. In this case, the authors propose the use of "phenomenological risk assessment" [59] to assign a very conservative probability of failure to the patch and use this to redefine the limit load for the unrepaired structure. By this method, the repaired structure with an intact patch must be capable of carrying the full limit load, but in the unlikely event of a poorly bonded repair, the underlying structure must be shown to be capable of withstanding the reduced limit load without a patch. The resulting level of safety would still be much higher than the original design, because a very conservative probability was used to generate the reduced limit load. By the tenets of phenomenological risk assessment, a conservative probability is assigned to the likelihood of failure based on expert opinion and regulatory acceptance. If it can be agreed upon that the likelihood of a bond lacking durability is much less than 1 in 100, then that is the likelihood that will be used. Whatever probability is chosen, service experience should be used as a basis for verification when possible. This probability can then be used to redefine the limit load for the unrepaired structure to give credit to the patch. If a gust load case were critical, this would lead to the critical case being defined as the gust that will occur 100 times during the life of the structure. This is consistent with providing a reasonable "get home" ability to the unrepaired structure and would work well with the requirement for a once-per-flight visual check of the patch. The authors will refer to this new process of reevaluation of the limit loads as "probabilistic load assessment."

Quadrant D requires a more detailed assessment of a repair design according to the process shown in Fig. 22. In quadrant D, the adhesive/composite stresses exceed the stress-based design criteria and the damage in the underlying structure is sufficient to require that the patch be credited in some manner to establish a useful life for the repair. Here, the methods used for damage-tolerance substantiation in quadrants A, B, and C are extended and we find additional requirements imposed for static or fatigue testing, comprehensive damage-tolerance analysis, and increased frequency and rigor in inspections, each depending on the particulars of the repair scenario. The use of the methodology and its rationale will be demonstrated by examining two scenarios.

The simplest scenario is one in which both the adhesive stresses and the residual strength of the structure may be addressed by the methods described for quadrants B and C. Here, we allow the removal of only one of the many factors leading to the certification of the adhesive and composite by compounded conservatism (e.g., reassessment of the fatigue loads or the environmental knockdown factor), with the understanding that the likelihood of a patch lacking durability is also very conservative and, accordingly, the resulting structure will still be much safer than the original design. If probabilistic load assessment is not sufficient and it is required to directly credit the patch to obtain an acceptable life, then additional testing and inspection requirements arise as shown.

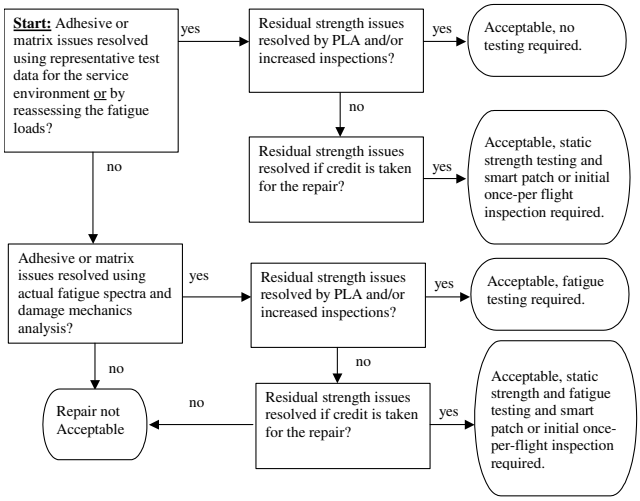

Fig. 22 Process for quadrant D repairs.

A more complex scenario is one in which an accurate damage-tolerance analysis of the repair is required to demonstrate adequate patch life. Here, we can no longer rely on simple stress-based criteria for the composite and adhesive, and a detailed fracture mechanics and fatigue analysis under the actual fatigue spectrum is required. Depending upon the residual strength of the structure, we find that a patch can be deemed to be outright unacceptable or acceptable with possibly onerous inspection and testing requirements. In this case, we have essentially reverted to the full requirements for certification of composite structures and detailed testing and analysis are required. Such a repair is likely to be uneconomical unless it is a fleet-wide repair or is to be applied to an integral component of the aircraft that cannot be removed or replaced.

VII. Conclusions

The experimental and finite element results clearly demonstrate the importance of both bending and cracked-plate geometry on the mechanics of a bonded composite repair. Even with a honeycomb bending restraint, bending strains in the repair were shown to be very significant. For an unrestrained repair, bending strains were shown to be dominant. The experimental results show a very large increase in the rate of failure and a change in failure mode when the honeycomb bending restraint is removed. A comparison of the finite element results with the failure criteria available in the open literature shows that adhesive tensile pressurization (closely linked to peel stresses) has a very large role in the failure of the patch in the unrestrained condition. Because bending plays such a critical role in the peel loading of the adhesive and failure of fibers in the patch, it is critical to fully include bending effects in the damage-tolerance assessment of single-sided or unbalanced repairs.

It was also demonstrated that hot and wet adhesive static strength is the critical case for both the adhesive and the composite matrix and should provide adequate protection against premature failure due to fracture, fatigue, and environmental effects. Accordingly, an adhesive allowable-stress approach was proposed (based on the work of Ignjatovic et al. [26]) that should reduce the requirements for the analysis of fatigue, fracture, and environmental effects. Because the method places a large penalty upon peel stresses, it should be adequate to protect against poor designs and thus reduce the need for testing during the certification of new repairs. Although more test data are required to characterize the FM73M adhesive (ideally, using a consistent method to determine the strain energy release rates) and the effect of adhesive thickness on fracture and fatigue thresholds needs to be assessed with rigor, this approach to adhesive characterization is promising and could expedite the certification of bonded joints.

Finally, the authors proposed a quadrant classification scheme for repairs, based upon the residual strength of the unrepaired structure and the calculated adhesive and composite stresses. Different

damage-tolerance analysis methods and requirements for substantiation were outlined for each class of repair. Because most day-to-day repairs of scratches, dents, oversized holes, and minor corrosion grind-outs should fall within quadrant A, rapid design and certification should be possible without much more engineering effort than is required for conventional riveted repairs. For other repairs, requirements for testing of representative specimens and in-service inspection are assigned by applying probabilistic risk assessment and the principle of compounded conservatism. The authors are hopeful that this new framework will enable much wider use of bonded composite repairs.

Acknowledgments

Additional funding for this work was provided through the Discovery Grant Research Program by the Natural Sciences and Engineering Research Council of Canada (NSERC) to Douglas P. Romilly. The authors thank the technical staff of the National Research Council of Canada Institute for Aerospace Research (NRC-IAR) for the painstaking work on the instrumentation of the specimen used in this study and Donald Raizenne for his assistance and advice.

References

[1] Baker, A. A., "Repair Efficiency in Fatigue-Cracked Aluminum Components Reinforced with Boron/Epoxy Patches," *Fatigue and Fracture of Engineering Materials and Structures*, Vol. 16, No. 7, 1993, pp. 753–765. doi:10.1111/j.1460-2695.1993.tb00117.x

[2] Baker, A. A., "Fiber Composite Repair of Cracked Metallic Aircraft Components—Practical and Basic Aspects," *Composites*, Vol. 18, No. 4, 1987, pp. 293–308. doi:10.1016/0010-4361(87)90293-X

[3] Baker, A. A., "Bonded Composite Repair of Metallic Aircraft Components—Overview of Australian Activities," *Composite Repairs of Military Aircraft Structures*, AGARD Conference Proceedings, CP-550, AGARD, Neuilly sur-Seine, France, 1994, pp. 1–14.

[4] Baker, A. A., Roberts, J. D., and Rose, L. R. F., "Experimental Study of Overlap Joint Parameters Relevant to K Reduction Due to Crack Patching," *28th National SAMPE Symposium*, Society for the Advancement of Material and Process Engineering, Covina, CA, 1983, pp. 1-1–1-12.

[5] Raizenne, M. D., Benak, T. J., Heath, J. B. R., Simpson, D. L., and Baker, A. A., "Bonded Composite Repair of Thin Metallic Materials: Variable Load Amplitude and Temperature Cycling Effects," *Composite Repairs of Military Aircraft Structures*, AGARD Conference Proceedings, CP-550, AGARD, Neuilly sur-Seine, France, 1994, pp. 5-1–5-12.

[6] Hucalek, P., Raizenne, M. D., and Scott, R. F., "Influences of Environment and Stress History on the composite Patch Repair of Cracked Metallic Structures," *Canadian Aeronautics and Space Journal*, Vol. 34, No. 2, 1988, pp. 85–91.

[7] Albat, A. M., Romilly, D. P., and Raizenne, M. D., "Thermal Residual Strain Measurement in a Composite Repair on a Cracked Aluminum Structure," *Proceedings of ICCM-11*, Australian Composite Structures Society, Melbourne, Australia, 14–18 July 1997, pp. VI-279–VI-288.

[8] Chalkley, P. D., Wang, C. H., and Baker, A. A., "Fatigue Testing of Generic Bonded Joints," *Advances in the Bonded Composite Repair of Metallic Aircraft Structure*, Vol. 1, edited by Baker, A. A., Rose, L. R. F., and Jones R., Elsevier, New York, 2002, pp. 103–136.

[9] Sharp, P. K., Clayton, J. Q., and Clark, G., "Retardation and Repair of Fatigue Cracks by Adhesive Infiltration," *Fatigue and Fracture of Engineering Materials and Structures*, Vol. 20, No. 4, 1997, pp. 605–614. doi:10.1111/j.1460-2695.1997.tb00292.x

[10] Poole, P., Lock, D., and Young, A., "Composite Patch Repair of Thick Aluminum Sections," *International Conference on Aircraft Damage Assessment and Repair*, Australian Inst. of Engineers, Barton, ACT, Australia, Aug. 1991, pp. 85–91.

[11] Denney, J., and Mall, S., "Characterization of Disbond Effects on Fatigue Crack Growth Behavior in Aluminum Plate with Bonded Composite Patch," *Engineering Fracture Mechanics*, Vol. 57, No. 5, 1997, pp. 507–525. doi:10.1016/S0013-7944(97)00050-7

[12] Denney, J., and Mall, S., "Fatigue behavior in Thick Aluminum Panels with a Composite Repair," *39th AIAA/ASME/ASCE/AHS/ASC Structures, Structural Dynamics, and Materials Conference*, Pt. 3, AIAA, Reston, VA, 1998, pp. 2434–2443.

[13] Denney, J., and Mall, S., "Effect of Disbond on Fatigue Behavior of Cracked Aluminum Panel with Bonded Composite Patch," *37th AIAA/ASME/ASCE/AHS/ASC Structures, Structural Dynamics & Materials Conferences*, Pt. 1, AIAA, Reston, VA, 1996, pp. 14–21.

[14] Klug, J., Malley, S., and Sun, C. T., "Characterization of Fatigue Behavior of Bonded Composite Repairs," *Journal of Aircraft*, Vol. 36, No. 6, 1999, pp. 1016–1022.

[15] Sabelkin, V., Mall, S., and Avram, J. B., "Fatigue Crack Growth Analysis of Stiffened Cracked Panel Repaired with Bonded Composite Patch," *Engineering Fracture Mechanics*, Vol. 73, No. 11, 2006, 1553–1567.

[16] Jones, R., Chiu, W. K., and Smith, R., "Airworthiness of Composite Repairs: Failure Mechanisms," *Engineering Failure Analysis*, Vol. 2, No. 2, 1995, pp. 117–128. doi:10.1016/1350-6307(95)00011-E

[17] Wojnar, R. T., "Damage Tolerance and Fatigue Evaluation of Structure," Advisory Circular No. 25.571-1C, Federal Aviation Administration, 29 Apr. 1998.

[18] Clark, R. J., "Damage Tolerance of Bonded Composite Repairs for Cracked Metallic Aircraft Structures," Ph.D. Thesis, Univ. of British Columbia, Vancouver, Apr. 2007.

[19] ANSYS University Intermediate, Software Package, Ver. 9.0, ANSYS, Inc., Canonsburg, PA, 2004.

[20] Albat, A. M., "Thermal Residual Stresses in Bonded Composite Repairs on Cracked Metal Structures," Ph.D. Thesis, Univ. of British Columbia, Vancouver, Sept. 1998

[21] Chalkley, P., and Baker, A. A., "Adhesives Characterization and Database," *Advances in the Bonded Composite Repair of Metallic Aircraft Structure*, Vol. 1, edited by A. A. Baker, Rose, L. R. F., and Jones, R., Elsevier, New York, 2002, pp. 87–102, Chap. 4.

[22] Anon., *Metallic Materials Properties Development and Standardization Handbook*, Federal Aviation Administration Rept. MMPDS-03 (formerly MIL-HDBK-5), 2006.

[23] NASGRO, Software Package, Ver. 4.0, Southwest Research Inst., San Antonio, TX, 2002.

[24] Duong, C. N., and Wang, C. H., "On the Characterization of Fatigue Crack Growth in a Plate with a Single-Sided Repair," *Journal of Engineering Materials and Technology*, Vol. 126, Apr. 2004, pp. 192–198. doi:10.1115/1.1647129

[25] Chalkley, P., and van den Berg, J., "On Obtaining Design Allowables for Adhesives Used in the Bonded Composite Repair of Aircraft," Australian Department of Defense, Defense Science and Technology Organization, Rept. DSTO-TR-0608, 1998.

[26] Ignjatovic, M., Chalkley, P., and Wang, C., "The Yield Behavior of a Structural Adhesive Under Complex Loading," Australian Department of Defense, Defense Science and Technology Organization, Rept. DSTO-TR-0728, 1998.

[27] Wang, C. H., and Chalkley, P., "Plastic Yielding of a Film Adhesive Under Multiaxial Stresses," *International Journal of Adhesion and Adhesives*," Vol. 20, No. 2, 2000, pp. 155–164. doi:10.1016/S0143-7496(99)00033-0

[28] Chester, R. J., Walker, K. F., and Chalkley, P. D., "Adhesively Bonded Repairs to Primary Aircraft Structure," *International Journal of Adhesion and Adhesives*, Vol. 19, No. 1, 1999, pp. 1–8. doi:10.1016/S0143-7496(98)00014-1

[29] Wilkins, D. J., Eisenmann, J. R., Camin, R. A., Margolis, W. S., and Benson, R. A., "Characterizing Delamination Growth in Graphite-Epoxy," *Damage in Composite Materials*, ASTM STP 775, edited by K. L. Reifsnider, American Society for Testing and Materials, Philadelphia, 1982, pp. 168–183.

[30] Lin, C., and Liechti, K. M., "Similarity Concepts in the Fatigue Fracture of Adhesively Bonded Joints," *Journal of Adhesion Science and Technology*, Vol. 21, No. 1, 1987, pp. 1–24. doi:10.1080/00218468708074956

[31] Hart-Smith, L. J., "Adhesively Bonded Double Lap Joints," NASA CR-112235, Jan. 1973.

[32] Mall, S., Johnson, W. S., and Everett, R. A., "Cyclic Debonding of Adhesively Bonded Composites," *Adhesive Joints: Formation, Characteristics, and Testing*, Plenum, New York1982, pp. 639–658.

[33] Kinloch, A. J., and Osiyemi, S. O., "Predicting the Fatigue Life of Adhesively-Bonded Joints," *The Journal of Adhesion*, Vol. 43, No. 1, 1993, pp. 79–90. doi:10.1080/00218469308026589

[34] Fernlund, G., Papini, M., McCammond, D., and Spelt, J. K., "Fracture Load Predictions for Adhesive Joints," *Composites Science and Technology*, Vol. 51, No. 4, 1994, 587–600.

[35] Williams, J. G., "On the Calculation of Energy Release Rates for Cracked Laminates," *International Journal of Fracture*, Vol. 36, No. 2, 1988, pp. 101–119. doi:10.1007/BF00017790

[36] Mall, S., Ramamurthy, G., and Rezaizdeh, M. A., "Stress Ratio Effect on Cyclic Debonding in Adhesively Bonded Composite Joints," *Composite Structures*, Vol. 8, No. 1, 1987, pp. 31–45. doi:10.1016/0263-8223(87)90014-6

[37] Mall, S., and Yun, K. T., "Effect of Adhesive Ductility on Cyclic Debond Mechanism in Composite-to-Composite Bonded Joints," *The Journal of Adhesion*, Vol. 23, No. 4, 1987, pp. 215–231. doi:10.1080/00218468708075408

[38] Mall, S., and Johnson, W. S., "Characterization of Mode 1 and Mixed-Mode Failure of Adhesive Bonds Between Composite Adherends," *Composite Materials: Testing and Design (Seventh Conference)*, ASTM STP 893, edited by J. M. Whitney, American Society for Testing and Materials, Philadelphia, 1986, pp. 322–334.

[39] Hwu, C., Kao, C. J., and Chang, L. E., "Delamination Failure Criteria for Composite Laminates," *Journal of Composite Materials*, Vol. 29, No. 15, 1995, pp. 1962–1987. doi:10.1177/002199839502901502

[40] Valentin, R. V., Butkus, L. M., and Johnson, W. S., "A Finite Element and Experimental Evaluation of Boron-Epoxy Doublers Bonded to an Aluminum Substrate," *Journal of Composites Technology and Research*, Vol. 20, No. 2, 1998, pp. 108–119.

[41] Butkus, L. M., and Johnson, W. S., "Environmental Effects on the Opening Mode Fracture Behavior of Bonded Boron-Epoxy/Aluminum Joints," *Proceedings of the American Society for Composites, Eleventh Technical Conference*, Technomic, Lancaster, PA, 7–9 Oct. 1996, pp. 1039–1048.

[42] Lubke, K. A., Butkus, L. M., and Johnson, W. S., "Effects of Environment on Fracture Toughness and Debond Growth of Aluminum/Fm73/Boron-Epoxy Adhesively Bonded Joints," *Journal of Composites Technology and Research*, Vol. 23, No. 1, 200, pp. 42–49.

[43] Johnson, W. S., "Stress Analysis of the Cracked-Lap-Shear Specimen: an ASTM Round-Robin," *Journal of Testing and Evaluation*, Vol. 15, No. 6, 1987, pp. 303–324. doi:10.1520/JTE11028J

[44] Rice, J. C., "Stresses in an Infinite Strip Containing a Semi-Infinite Crack," *Journal of Applied Mechanics*, Vol. 33, No. 2, 1967, pp. 248–249.

[45] Krenk, S., "Energy Release Rate of Symmetric Adhesive Joints," *Engineering Fracture Mechanics*, Vol. 43, No. 4, 1992, pp. 549–559. doi:10.1016/0013-7944(92)90198-N

[46] Hart-Smith, L. J., "Design and Analysis of Bonded Repairs for Metal Aircraft Structures," *Bonded Repair of Aircraft Structures*, edited by Baker A. A., and Jones, R., Martinus Nijhoff, Dordrecht, The Netherlands, 1988, pp. 31–47.

[47] Cheulk, P. T., Tong, L., Wang, C. H., Baker, A., and Chalkley, P., "Fatigue Crack Growth in Adhesively Bonded Composite-Metal Double-Lap Joints," *Composite Structures*, Vol. 57, No. 1, 2002, pp. 109–115. doi:10.1016/S0263-8223(02)00074-0

[48] Anon., *Composite Materials Handbook—MIL 17*, Vol. 3, MIL-HDBK-17-3F, American Society for Testing and Materials, West Conshohocken, PA, 2002.

[49] Hull, D., and Cliyne, T. W., "An Introduction to Composite Materials," 2nd ed., Cambridge Univ. Press, Cambridge, MA, 1996.

[50] Pipes, R. B., "On the Off-Axis Strength of Anisotropic Materials," *Journal of Composite Materials*, Vol. 7, No. 2, 1973, pp. 246–256. doi:10.1177/002199837300700208

[51] Hashin, Z., "Failure Criteria for Unidirectional Fiber Composites," *Journal of Applied Mechanics*, Vol. 47, June 1980, pp. 329–334.

[52] Sodena, P. D., Kaddour, A. S., and Hinton, M. J., "Recommendations for Designers and Researchers Resulting from the World-Wide Failure Exercise," *Composites Science and Technology*, Vol. 64, No. 3, Mar. 2004, pp. 589–604. doi:10.1016/S0266-3538(03)00228-8

[53] Hart-Smith, L. J., "What Textbooks Won't Teach You About Interactive Composite Failure Criteria," *Composite Structures: Theory and Practice*, ASTM STP 1383, edited by P. Grant and, C. Q. Rousseau, American Society for Testing and Materials, West Conshohocken, PA, 2000, pp. 413–436.

[54] Papikanos, P., Tserpes, K. I., Labeas, G., and Pantelakis, Sp., "Progressive Damage Modeling of Bonded Composite Repairs," *Theoretical and Applied Fracture Mechanics*, Vol. 43, No. 2, 2005, pp. 189–198. doi:10.1016/j.tafmec.2005.01.004

[55] Clark, R. J., and Romilly, D. P., "Linear Coupled Bending and Extension of an Unbalanced Bonded Composite Repair," *International Journal of Solids and Structures*, Vol. 44, No. 10, 2007, pp. 3156–3176. doi:10.1016/j.ijsolstr.2006.09.012

[56] Clark, R. J., and Romilly, D. P., "Nonlinear Mechanics of Hybrid Bonded Joints and Bonded Composite Repairs," *International Journal of Nonlinear Mechanics* (submitted for publication).

[57] Clark, R. J., and Romilly, D. P., "Fatigue Damage Prediction for Bonded Composite Repairs Applied to Metallic Aircraft Structures," Society of Automotive Engineers, Paper 2001-01-2628, 2001.

[58] Okafor, A., Singh, N., Enemuoh, U. E., and Rao, S. V., "Design, Analysis and Performance of Adhesively Bonded Composite Patch Repair of Cracked Aluminum Aircraft Panels," *Composite Structures*, Vol. 71, No. 2, 2005, pp. 258–270. doi:10.1016/j.compstruct.2005.02.023

[59] Theofanous, T. G., "On the Proper Formulation of Safety Goals and Assessment of Safety Margins for Rare and High-Consequence Hazards," *Reliability Engineering & System Safety*, Vol. 54, Nos. 2–3, 1996, pp. 243–257. doi:10.1016/S0951-8320(96)00079-8

[60] Baker, A. A., "On the Certification of Bonded Composite Repairs to Primary Aircraft Structure," *Proceedings of ICCM-11*, Australian Composite Structures Society, Melbourne, Australia, 1997, pp. I-1 to I-23.